New Journal of Physics
The open access journal at the forefront of physics
Deutsche Physikalische Gesellschaft DPG | IOP Institute of Physics

Phase-resolved measurement of the spatial surface charge distribution in a laterally patterned barrier discharge

R Wild and L Stollenwerk

Institute of Physics, University of Greifswald, Felix-Hausdorff-Str. 6, D-17487 Greifswald, Germany
E-mail: wild@physik.uni-greifswald.de and stollenwerk@physik.uni-greifswald.de

Received 22 May 2014, revised 11 September 2014
Accepted for publication 7 October 2014
Published 20 November 2014

New Journal of Physics **16** (2014) 113040

doi:10.1088/1367-2630/16/11/113040

Abstract

The presented experimental system is a barrier discharge system with plane parallel electrodes. The lateral surface charge distribution being deposited on the dielectric layer during each breakdown is observed optically using the well known electro-optic effect (Pockels effect). The temporal resolution of the surface charge measurement has been increased to 200 ns, and so for the first time it is possible to resolve the charge transfer to the dielectric surface in a single breakdown. In the present measurements, a patterned glow-like barrier discharge is investigated. It is found that the charge reversal in a single discharge spot (microdischarge) starts in the centre and then grows outwards. These experimental findings verify previously unconfirmed predictions from earlier numerical calculations and thereby contribute to a better understanding of the interaction between the plasma and the electrical charge on the electrodes.

Keywords: barrier discharge, phase resolved surface charge measurement, numerical simulation, discharge evolution

1. Introduction

Dielectric barrier discharges (BD) are important and well-used plasma sources. The barrier inside the discharge volume prevents high-current arcing, therefore this plasma source a good candidate for applications at low-temperatures, such as plasma display panels [1], surface modification [2] and use in the biomedical sector [3, 4]. The measurement of surface charge deposited on the dielectric surface has recently gained attention because of its significant contribution to the overall behaviour of the discharge [5, 6]. A measurement with a high temporal resolution is especially desirable because the deposition mechanism of the surface charge endures only a fraction of the discharge cycle. Until now, the temporal resolution of the surface charge measurement has been too coarse to resolve a single breakdown in a laterally structured barrier discharge, thus, only breakdowns in diffuse discharges have been investigated and temporally resolved [6]. The best temporal resolution of the optical surface charge measurement obtained up to now is 600 ns in a plasma jet setup [7]. In the present work the temporal resolution is further increased. Hence, for the first time, a phase resolved surface charge measurement in a patterned barrier discharge is possible, being able to image the charge transfer within a single breakdown. The measurements presented in this article confirm the temporal behaviour of the charge deposition process that has been predicted by numerical simulations in [8].

The patterned barrier discharge under consideration in this work is observed in planar electrode arrangements with a high aspect ratio, i. e., with a small discharge gap compared to the lateral extension. Contrary to fast micro discharges that follow a streamer mechanism (as observed in [9, 10]), they behave electrically in a way usually observed in diffuse glow-like discharges (as observed in [11, 12]); the current pulse duration is in the microsecond range and the current density is several $\mathrm{mA\,cm^{-2}}$. However, in contrast to common glow-like barrier discharges, within some ten periods of the driving voltage the discharge becomes laterally patterned, i. e., split up into several discharge spots [13]. Through variation of the amplitude of the driving voltage the number of spots can be changed [8, 14]. Often, the discharge spots move across the discharge area and come to a rest after few minutes [15]. Laterally patterned discharges have been observed by several other authors, e. g. [14, 16–20]. Mostly, they appear in helium or helium mixtures in the parameter range of pressure p from 75 to 1000 hPa, frequency f from 50 to 200 kHz, electrode distance d from 0.5 to 3 mm, voltage $\hat{U}$ from 300 to 800 V.

2. Experimental setup

The discharge cell consists of two electrodes at a distance of $d = 0.7$mm from each other. The first electrode is a dielectric bismuth silicon oxide (BSO) crystal (width: $a_{\mathrm{BSO}} = 0.5$ mm) that is on top of a grounded aluminium mirror. The second electrode is an indium tin oxide (ITO) coated glass plate with its electrically conducting side pointing to the gas gap. A sinusoidal voltage with a frequency of $f = 100$kHz is applied to the electrodes. The discharge is operated with helium at a pressure of $p = 100$hPa. For each measurement, the discharge is started with an applied voltage of approximately 250 V. The discharge area is then completely filled with moving discharge spots. In order to safely distinguish between the spots, their number is

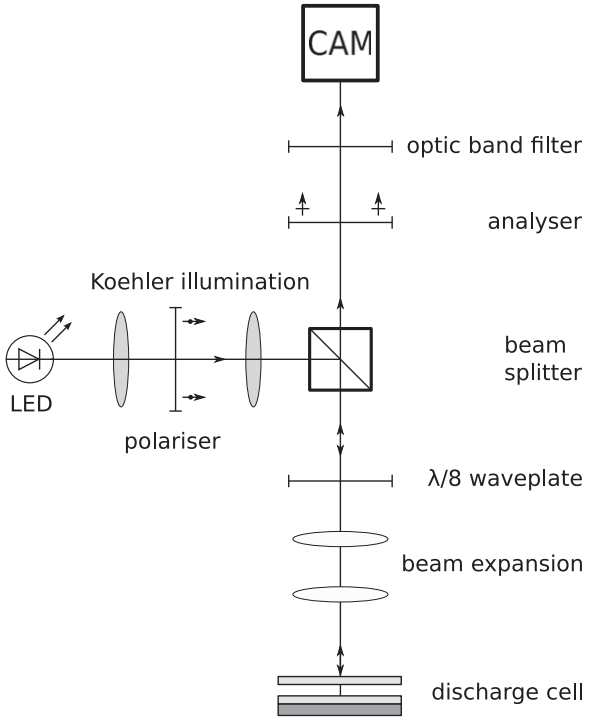

Figure 1. Sketch of the experimental setup.

reduced by lowering the applied voltage to $U_{\mathrm{app}} = 200$ V. When the discharge spots have become stationary after a few minutes, the measurement is started.

The surface charge measurement is based on the polarisation shift of light that passes through the BSO crystal. Its optical properties cause a birefringence that is proportional to the electric field applied to the crystal. The electric field originating from surface charge on the BSO dielectric is measured with a setup sketched in figure 1. The light emitted by an LED ($\lambda = 638$ nm) becomes linearly polarised. From the beam splitter, it is reflected by the aluminium mirror and finally passes an analyser in front of the camera. On its way, it is retarded by twice the phase retardation from the $\lambda/8$-wave plate and the additional phase shift $\Delta\Phi$ according to the voltage drop U over the BSO crystal, with

$$\Delta\Phi = \frac{2\pi}{\lambda}\, n_0^3\, r_{41}\, U = kU. \tag{1}$$

In equation (1), n_0 is the undisturbed refraction index ($n_0 = 2.54$) of BSO, and r_{41} is its electro-optic constant that has been determined as 2.4 pm V^{-1} in a calibration measurement. The analyser in front of the high speed camera (Phantom Miro) is orientated perpendicular to the initial polariser. An optic band filter in front of the camera ensures that only the light emitted from the LED is detected. The intensity in front of the camera $I(U)$ is expressed as

$$I(U) = I_0 \left| \frac{1}{2}\left(\exp\left\{ \mathrm{i}\left(\frac{\pi}{2} + 2\Delta\Phi(U) \right) \right\} - 1 \right) \right|^2. \tag{2}$$

Here, I_0 is the intensity of the light of the LED. In linear approximation, equation (2) becomes

$$I(U) = I_0\left(\frac{1}{2} + kU\right). \tag{3}$$

Based on equation 3, let us define two intensities that correspond to characteristic situations during the measurement. The first is a surface charge free reference intensity I_r, where an external voltage drop U_r on the BSO may be across the crystal, with

$$I_\mathrm{r} = I_0\left(\frac{1}{2} + kU_\mathrm{r}\right). \tag{4}$$

The other intensity corresponds to the actual measurement, where the voltage comprises of a contribution from the surface charge U_σ as well as from external voltage U_m, hence

$$I_\mathrm{m} = I_0\left[\frac{1}{2} + k\left(U_\sigma + U_\mathrm{m}\right)\right]. \tag{5}$$

To compute the voltage contribution U_σ of the surface charge, the ratio $I_\mathrm{m}/I_\mathrm{r}$ is formed and resolved for U_σ:

$$U_\sigma = \left[\frac{I_\mathrm{m}}{I_\mathrm{r}}\left(1 + 2kU_\mathrm{r}\right) - 1\right]\frac{1}{2k} - U_\mathrm{m} \tag{6}$$

Finally, the voltage U_σ can be converted to the corresponding surface charge density sigma assuming a parallel-plate capacitor:

$$\sigma = U_\sigma \frac{\varepsilon_0 \varepsilon_\mathrm{BSO}}{a_\mathrm{BSO}}, \tag{7}$$

with a thickness of the BSO crystal of $a_\mathrm{BSO} = 0.5\,\mathrm{mm}$, a dielectric constant of BSO of $\varepsilon_\mathrm{BSO} = 56$, and ε_0 being the vacuum permittivity. In the measurements presented in this article, the reference image is recorded without external voltage (i. e. $U_\mathrm{r} = 0$), thus equation (7) becomes

$$\sigma(x, y) = \frac{\varepsilon_0\ \varepsilon_\mathrm{BSO}}{a_\mathrm{BSO}} \cdot \left[\frac{\lambda}{4\pi\ n_0^3\ r_{41}}\left(\frac{I_\mathrm{m}(x, y)}{I_\mathrm{r}(x, y)} - 1\right) - U_\mathrm{m}\right]. \tag{8}$$

In order to provide a temporal resolution of the measurement, the light coming from the LED is pulsed synchronously to the discharge driving voltage ($f_\mathrm{LED} = 100$ kHz) with one pulse per cycle. The camera has an exposure time of $t_\mathrm{exp} = 2\mathrm{ms}$, so every camera frame averages over 200 LED pulses. To reduce the noise, 50 frames are recorded under the same conditions and averaged. Then, the LED pulse is shifted by $\Delta t = 200\,\mathrm{ns}$ relative to the discharge driving voltage and a new measurement cycle starts. The pulse width of one LED pulse is $t_\mathrm{LED} = 400\mathrm{ns}$, so subsequent measurements overlap by 50% in time. The shape of the light intensity of an LED pulse is shown in figure 2. It can be approximated as a square pulse.

3. Experimental results

In figure 3, the phase resolved development of the surface charge density along with the driving voltage and the current form is shown. The value for the surface charge represents an average over the whole BSO surface. In each half period of the applied voltage, one breakdown occurs.

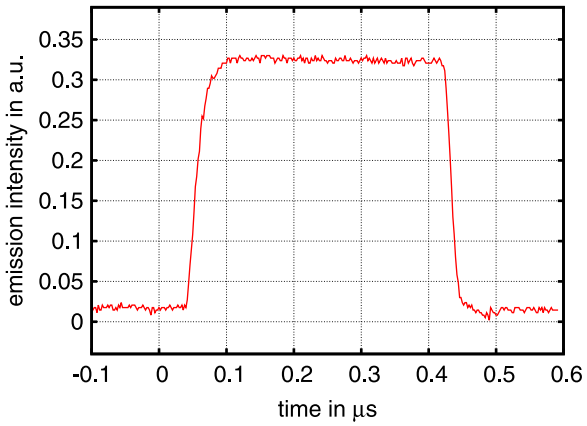

Figure 2. Profile of the light emission of the LED during one light pulse. The origin of the time axis corresponds to the trigger event for the LED controller.

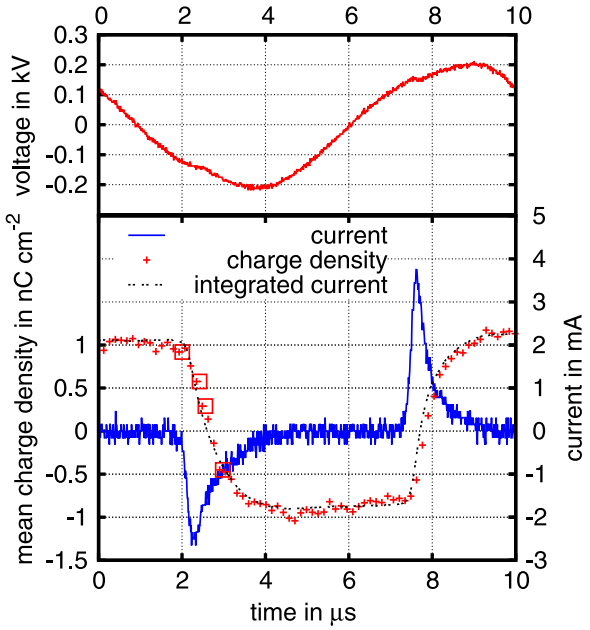

Figure 3. Development of voltage, real current, and mean surface charge density during one period of the applied voltage. The charge represents the mean surface charge density of the whole BSO surface. The squares mark the selected times in figure 6.

The mean surface charge density changes its value and polarity according to the occurrence of a current pulse. It behaves like the integrated current, which is also shown in figure 3.

During each current pulse, a number of micro discharges are ignited simultaneously (figure 4(a)). Each micro discharge produces a surface charge spot as a 'footprint' that remains in the same position at least until the next discharge event (figures 4(b) and (c)). To examine the development of a charge spot for each temporal position, the surface charge density distribution is scanned for individual spots and cropped around them. From these croppings, a mean lateral surface charge density distribution for the spots is computed. In figure 5, the mean surface charge density distribution of a surface charge spot is shown for positive and negative polarity.

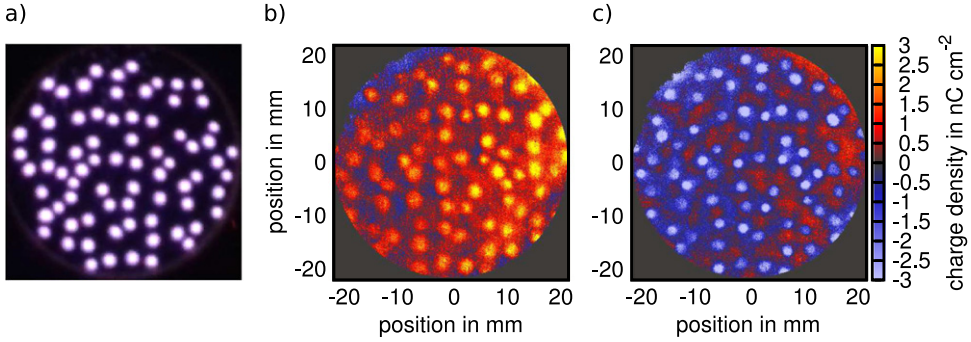

Figure 4. Overview of the whole electrode surface. (a) Photography of the discharge, (b) surface charge density distribution on the whole electrode at $t = 1.6\,\mu$s, (c) surface charge density distribution on the whole electrode at $t = 7.0\,\mu$s.

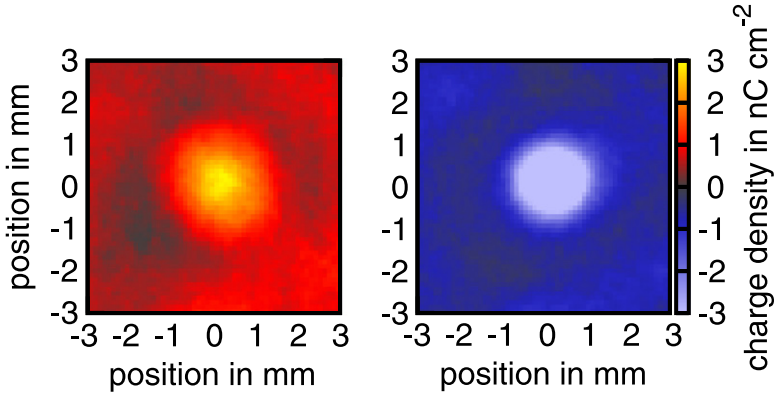

Figure 5. Mean surface charge density distribution for positive (left) and negative (right) polarity. The measurements were taken at $t = 1.6\,\mu$s and $t = 7.0\,\mu$s, when the charge density is temporally constant.

Both were taken during temporally constant conditions, i. e., with no discharge taking place. They represent the state of surface charge just before a discharge starts. The peak surface charge densities are $\sigma_+ = 2.7$ nC cm^{-2} for the positive peak, and $\sigma_- = -4.6$ nC cm^{-2} for the negative peak. Also, the spots are usually on a charge offset, with $\sigma_{\mathrm{off},+} = 0.5$ nC cm^{-2} for the positive polarity and $\sigma_{\mathrm{off},-} = -0.5$ nC cm^{-2} for the negative polarity.

In figure 6, a typical deposition process of negative charge is shown. Again, the charge distribution is averaged over all spots in the discharge area. In the beginning, at $t = 2.0\,\mu$s, there is a spot of positive surface charge, which has been deposited in the previous half-cycle. The charge profile through its centre is roughly Gaussian. During the charge deposition, the charge density is at first reduced globally, resulting in a shallower profile and a lower charge density offset (e. g. at $t = 2.4\,\mu$s). However, the lateral charge deposition rate is not constant, instead it is most intense at the centre of the spot. Eventually, this results in a local minimum enclosed between two maxima (at $t = 2.6\,\mu$s) in the charge density profile and the surface charge spot is successively radially replaced by its opposite charge. Finally, at $t = 3.0\,\mu$s, the charge profile reaches a state that is again roughly Gaussian, now for negative charge. Through the remaining low current density onto the dielectric surface, the charge distribution reaches the steady state as

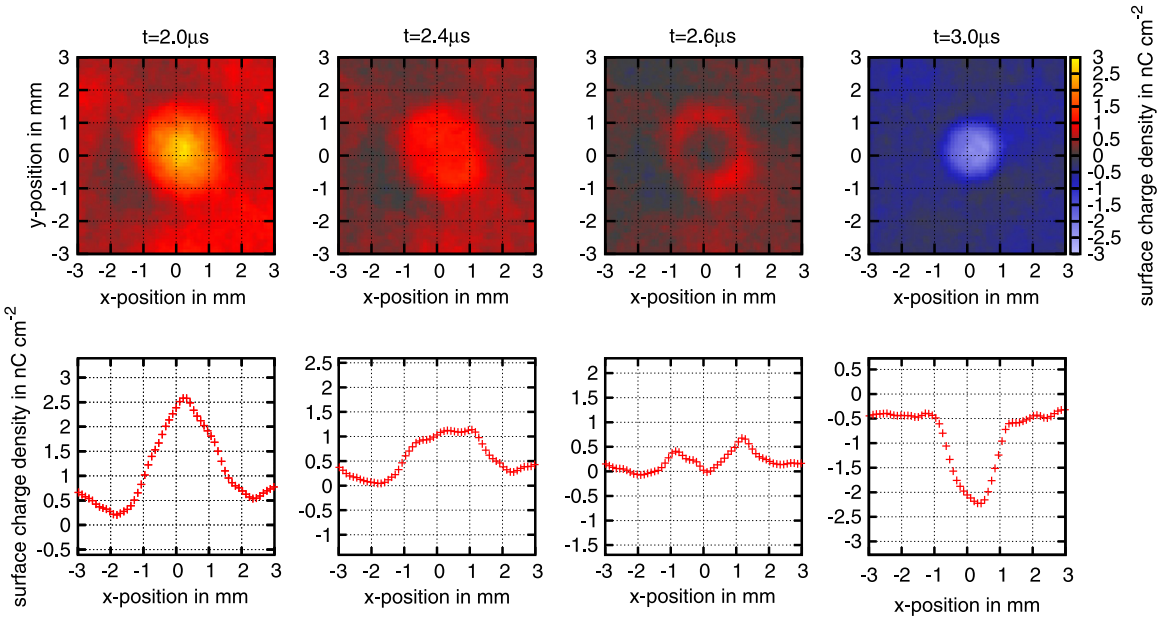

Figure 6. Charge deposition in a current spot during the breakdown in the negative half-cycle. The times of recording for the displayed snapshots are marked in figure 3. Upper row: charge distribution of an averaged current spot. Lower row: representative cross sections through the centre of the current spot.

it is shown in figure 5 for 7.0 μs. The process of positive charge deposition takes place analogously to the deposition of negative charge with reversed sign.

4. Comparison to numerical calculations

In the past, the only way to get insight into the development of the surface charge distribution in a laterally patterned discharge was to use theoretical considerations, mainly by numerical calculations. Therefore, we want to compare the newly found experimental results with previous numerical predictions. The memory effect induced by the surface charge spots has been well established theoretically and experimentally. However, the recharging of a charge spot starting in the centre and growing radially outwards is a newly discovered phenomenon that should also be reproduced in numerical simulations.

A numerical simulation of a single discharge spot in a plane parallel barrier discharge has been performed in [8] and the chosen physical parameters are similar to the present experiments. The underlying model is a simple drift-diffusion model comprising of continuity equations for electrons and singly charged ions as well as the Poisson equation for the electric field. The equations have been solved in three dimensions on a $60 \times 60 \times 60$ grid with zero flux boundary conditions with x being the direction perpendicular to the electrodes and y, z the plane parallel to the electrodes. To exploit the limited grid size efficiently, a quarter of a current spot has been placed into one corner of the discharge area. Through the mirroring effect of the zero flux boundary condition it is completed to a whole current spot.

The physical dimensions of the system under consideration are given by a discharge gap of $d = 0.5$ mm with both electrodes covered with a dielectric of thickness of $a = 0.5$ mm. The

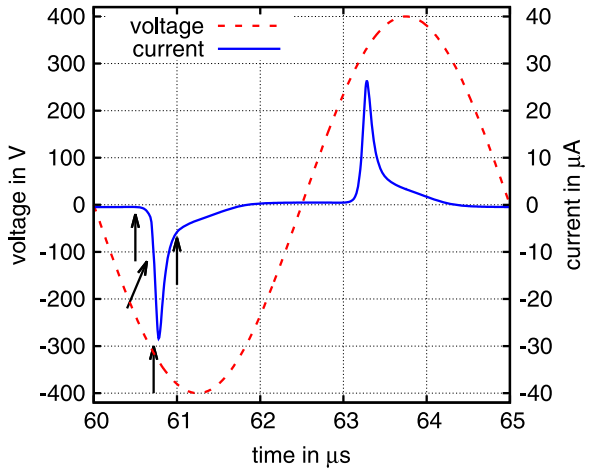

Figure 7. Driving voltage and real curent in the numerical simulation. The arrows depict the times of the graph in figure 8.

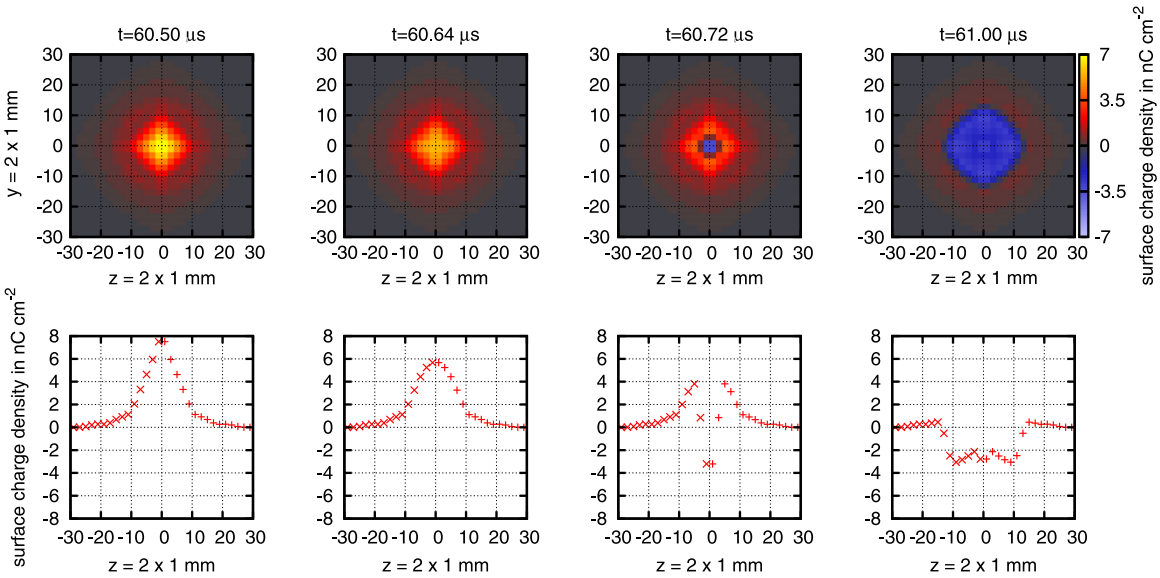

Figure 8. Charge deposition in a current spot during the breakdown in the negative half-cycle in a numerical simulation. The upper row shows the smoothed surface charge distribution on the dielectric for different times, the lower row shows a corresponding cut along the z-axis. According to the zero flux boundary conditions, all graphs are mirrored at the origin.

dielectric permittivity is $\varepsilon = 7.6$ and its secondary emission coefficient is $\gamma = 0.05$. The working gas is pure helium at a pressure of $p = 200\,\mathrm{hPa}$. The system is driven by a sinusoidal voltage with an amplitude of $\hat{U} = 400\mathrm{V}$ and a frequency of $f = 200\,\mathrm{kHz}$. The gas and ion temperature is set to 25 meV, the electron temperature is 2 eV.

Starting from an initial spot-like surface charge distribution, several breakdowns of the numerical simulation were run until a steady state was reached. In figure 7, the applied voltage and the real current in a steady state discharge are shown. The discharge type determined from the current shape fits very well to the experimental data shown in figure 3. From the

development of the electric field during the breakdown, the discharge type can be identified as a locally restricted glow-like discharge [8]. In figure 8, the development of the surface charge distribution during a single breakdown is shown. The relevant cutout of the numerical data has been mirrored at the boundaries in order to show the whole discharge spot, thus the diagrams in figure 8 are comparable to those in figure 6 for the experimental results. The times of the snapshots shown in figure 8 are marked in figure 7 with arrows, and as with the experimental results, the deposition of negative charge on the surface is shown. The initial surface charge density distribution (at $t = 60.50\,\mu$s) is quickly reduced in amplitude (at $t = 60.64\,\mu$s). The current density is highest in the centre of the spot, hence the surface charge density there is eventually negative even though its surrounding is still positively charged (at $t = 60.72\,\mu$s). Then, starting from the centre, the surface charge spot is radially replaced by negative charge. The breakdown with reversed polarity in the next half-period takes place qualitatively equally.

5. Conclusion

The high temporal resolution of the optical surface charge measurement presented in this article offers for the first time an insight into the charge development within a single breakdown of a patterned barrier discharge, i. e., the decrease and subsequent increase of surface charge in the course of a breakdown can be observed. On a global scale, regarding the overall discharge current from the electrical measurement and the spatially integrated surface charge from the optical measurement, a good quantitative agreement between the traditional electrical and the optical measurement is found. Regarding a single discharge spot laterally resolved, an interesting behaviour of the charge transfer was found: the charge reversal starts in the centre of a residual surface charge spot and grows radially outwards. The maximum of the real current peak coincides with a ring-shaped surface charge density distribution.

The experimental findings presented here support the predictions from previous numerical simulations. Although the discharge parameters are not equal they are very similar in the experiments and the numerical simulations, and both are well within the parameter range known for patterned discharges. From the simulation it is known that the discharge is started in the center of the surface charge spot because the electric field is highest there. While the discharge burns, a new, opposite charge is accumulated on the surface. Thus, the maximum of the electric field in the center of a discharge spot vanishes and instead a ring-shaped maximum with temporarily increasing radius emerges. As the current onto the dielectric surfaces moves along the electric field, the polarity of the charge spot is reversed starting from the center. In this way, the experimentally observed development of the surface charge distribution is qualitatively reproduced and comprehensible. Quantitatively, the numerical results are well within the same order of magnitude.

Acknowledgments

The authors are grateful to Uwe Meissner and Peter Druckrey for providing practical and technical assistance. This work was funded by the *Deutsche Forschungsgemeinschaft*, SFB TRR-24 (B14).

References

[1] Boeuf J-P 2003 Plasma display panels: physics, recent developments and key issues *J. Phys. D: Appl. Phys.* **36** 53–79

[2] Wagner H-E, Brandenburg R, Kozlov K V, Sonnenfeld A, Michel P and Behnke J F 2003 The barrier discharge *Vakuum* **71** 417–36

[3] Weltmann K D, Kindel E, Woedtke Th v, Hähnel M, Stieber M and Brandenburg R 2010 Atmospheric-pressure plasma sources: prospective tools for plasma medicine *Pure Appl. Chem.* **82** 1223–37

[4] von Woedtke T, Reuter S, Masur K and Weltmann K-D 2013 Plasmas for medicine *Phys. Rep.* **00** 1–38

[5] Massines F, Segur P, Gherardi N, Khamphan C and Ricard A 2003 Physics and chemistry in a glow dielectric barrier discharge at atmospheric pressure: diagnostics and modelling *Surf. Coat. Tech.* **174–175** 8–14

[6] Bogaczyk M, Wild R, Stollenwerk L and Wagner H-E 2012 Surface charge accumulation and discharge development in diffuse and filamentary barrier discharges operating in He, N_2 and mixtures *J. Phys. D: Appl. Phys.* **45** 465202

[7] Wild R, Gerling T, Bussiahn R, Weltmann K-D and Stollenwerk L 2014 Phase-resolved measurement of electric charge deposited by an atmospheric pressure plasma jet on a dielectric surface *J. Phys. D: Appl. Phys.* **47** 042001

[8] Stollenwerk L, Amiranashvili Sh, Boeuf J-P and Purwins H-G 2007 Formation and stabilisation of single current filaments in planar dielectric barrier discharge *Eur. Phys. J.* D **44** 133–9

[9] Kozlov K V, Wagner H-E, Brandenburg R and Michel P 2001 Spatio-temporally resolved spectroscopic diagnostics of the barrier discharge in air at atmospheric pressure *J. Phys. D: Appl. Phys.* **34** 3164–76

[10] Kogelschatz U 2003 Dielectric-barrier discharges: their history, discharge physics, and industrial applications *Plasma Chem. Plasma Process.* **23** 1–46

[11] Massines F, Rabehi A, Decomps P, Gadri R B, Segur P and Mayoux C 1998 Experimental and theoretical study of a glow discharge at atmospheric pressure controlled by dielectric barrier *J. Appl. Phys.* **83** 2950–7

[12] Gherardi N and Massines F 2001 Mechanisms controlling the transition from glow silent discharge to streamer discharge in nitrogen *IEEE Trans. Plasma Sci.* **29** 536–44

[13] Stollenwerk L, Amiranashvili S, Boeuf J-P and Purwins H-G 2006 Measurement and 3D simulation of self-organized filaments in a barrier discharge *Phys. Rev. Lett.* **96** 255001

[14] Wild R and Stollenwerk L 2012 Breakdown of order in a self-organised barrier discharge *Eur. Phys. J.* D **66** 214–9

[15] Stollenwerk L, Amiranashvili S and Purwins H-G 2006 Forced random walks with memory in a glow mode dielectric barrier discharge *New J. Phys.* **8** 217

[16] Boyers D B and Tiller W A 1982 Plasma bubble domains: a magnetic bubble analog *Appl. Phys. Lett.* **41** 28–31

[17] Breazeal W, Flynn K M and Gwinn E 1995 Static and dynamic two-dimensional patterns in self-extinguishing discharge avalanches *Phys. Rev.* E **52** 1503–19

[18] Brauer I, Bode M, Ammelt E and Purwins H-G 2000 Traveling pairs of spots in a periodically driven gas discharge system: collective motion caused by interaction *Phys. Rev. Lett.* **84** 4104–7

[19] Zanin A L, Gurevich E L, Moskalenko A S, Bödeker H U and Purwins H-G 2004 Rotating hexagonal pattern in a dielectric barrier discharge system *Phys. Rev.* E **70** 036202

[20] Dong L, Liu W, Wang H, He Y, Fan W and Gao R 2007 Honeycomb hexagon pattern in dielectric barrier discharge *Phys. Rev.* E **76** 046210